Isolation of a *Drosophila* amplification origin developmentally activated by transcription

Fang Xie and Terry L. Orr-Weaver*

Whitehead Institute for Biomedical Research and Department of Biology, Massachusetts Institute of Technology, 9 Cambridge Center, Cambridge, MA 02142

Contributed by Terry L. Orr-Weaver, April 30, 2008 (sent for review February 14, 2008)

We exploited the *Drosophila* Amplicon in Follicle Cells, *DAFC-62D*, to identify a new metazoan amplification origin, *ori62*. In addition to the origin, *DAFC-62D* contains two other developmental stage-specific binding regions for the Origin Recognition Complex (ORC) and the replicative helicase MCM2–7. All three of these regions are required for proper amplification. There are two rounds of amplification initiation at *ori62*, and the second round is preceded by transcription across *ori62*. We show by α-amanitin inhibition that RNA polymerase II (RNAPII) transcription is required to localize MCM2–7 (but not ORC) to permit the second round of origin firing. This role for transcription appears unique to *DAFC-62D*, because neither other *DAFC*s nor ectopic transposons with the *DAFC-62D* replication elements bounded by functional chromatin insulators are affected by α-amanitin. By sequential chromatin immunoprecipitation, we show that the MCM complex and RNAPII are bound to the same 100–500 bp pieces of chromatin during late origin firing. These results raise the possibility that RNAPII may recruit MCM2–7 at some metazoan replication origins.

DNA replication | gene amplification | MCM | ORC | RNA polymerase II

Proper regulation of the initiation of DNA replication is crucial for cell division in eukaryotes. The first step of initiation is the selection of origins by the prereplicative complex (pre-RC), composed of the six-subunit origin recognition complex (ORC), Cdc6, Cdt1, and MCM2–7 (1). Although these protein factors are highly conserved, the DNA sequences that define origin activity in different organisms are not (2). With recent advances in DNA microarray technology, genome-wide mapping of replication origins has begun to establish the spatial and temporal program of replication initiation (3). However, the mechanisms of origin selection, especially in response to developmental cues in metazoans, remain poorly understood. Only a handful of model metazoan replicons have been studied in detail (2, 4). Furthermore, few observations of cell-type specific or developmental regulation of replication origins have been reported (5, 6).

Developmental gene amplification in the ovarian follicle cells of *Drosophila* provides a powerful system for the analysis of metazoan DNA replication and developmental regulation of origin firing (7, 8). Amplification occurs by repeated rounds of origin firing and bidirectional movement of replication forks from these origins to produce 100 kb gradients of amplified DNA (7). This process depends on the same replication initiation and elongation proteins necessary for genomic replication (7, 8). P-element mediated transformation experiments, facilitated by the use of insulators to buffer transposons from chromosomal position effects (9), have allowed dissection of *cis* regulatory elements required for amplification. In the well characterized third chromosome chorion amplicon, *DAFC-66D*, both an origin of replication (*ori*β) and a replication enhancer (*ACE3*) have been defined [for review see (8)]. *ACE3* stimulates replication from proximal origins and provides the developmental specificity for amplification by acting to load ORC, which appears to localize broadly across the amplicon, rather than strictly to the origin. ORC activity and origin firing at *DAFC-66D* are regulated by the transcription factors E2F1/RBF (10, 11) and the Myb protein complex (12, 13).

A newly identified amplicon, *DAFC-62D*, differs in its developmental timing from the other *DAFC*s (Fig. 1*A*), providing the opportunity to decipher how origin firing is influenced by differentiation events (14). The most abundantly amplified amplicon, *DAFC-66D*, undergoes approximately five rounds of origin activation, restricted to stages 10B and 11, to give an amplification level of 30–40 fold at the origin (15). There are no more initiation events during subsequent stages of follicle cell development, but only the elongation of previously formed replication forks continues (Fig. 1*A*). At *DAFC-62D*, amplification initiates only once in stage 10B, but in stage 13 there is an additional increase in copy number at a very precise region (14). We, therefore, investigated mechanisms that control the unique timing of *DAFC-62D* origin activation.

Results and Discussion

Identification of the Replication Origin and Pre-RC Binding Sites in *DAFC-62D*. To determine the site at which DNA synthesis initiates during amplification at *DAFC-62D*, nascent strand analysis was performed as described (16, 17) on replicative intermediates isolated from stage 10B or 13 egg chambers. We observed a 1 kb region that was highly enriched in the 0.5–1 kb (Fig. 1*B*) and 1–1.6 kb (data not shown) fractions of nascent DNA, thus containing origin activity in both stage 10B and 13. We have designated this region as *ori62*. As a control for the λ-exonuclease digestion and uniform efficiency of PCR, DNA of size 5 kb and above that was not expected to contain nascent strands displayed uniformly low levels across *DAFC-62D* (Fig. 1*B*). As a positive control, we found that the known origin *ori*β of *DAFC-66D* was enriched in the 0.5–1 kb fraction ≈14-fold over a locus 5 kb away (data not shown).

We used quantitative chromatin immunoprecipitation (ChIP) with antibodies against the ORC2 subunit (18) to test whether ORC was present at *ori62* and/or additional sequences, quantifying the amounts present by real-time PCR. ORC2 has been localized to *DAFC*s by immunofluorescence (10, 15) and also shown to be necessary for amplification, because a hypomorphic, female-sterile mutation in the *Drosophila orc2* gene causes reduced levels of amplification (19). In *DAFC-62D*, we detected significant localization of ORC to *ori62* by ChIP and real-time PCR quantification (Fig. 1*D*). In contrast to *ACE3* (Fig. 1*C*), ORC binding remained present in stages 12 and 13 at *ori62*, paralleling the fact that an additional round of amplification takes place at *DAFC-62D* in stage 13 (14).

In addition to *ori62*, ChIP on stage 10A, 12, and 13 egg

Author contributions: F.X. and T.L.O.-W. designed research; F.X. performed research; F.X. analyzed data; and F.X. and T.L.O.-W. wrote the paper.

The authors declare no conflict of interest.

Freely available online through the PNAS open access option.

*To whom correspondence should be addressed. E-mail: weaver@wi.mit.edu.

This article contains supporting information online at www.pnas.org/cgi/content/full/0804146105/DCSupplemental.

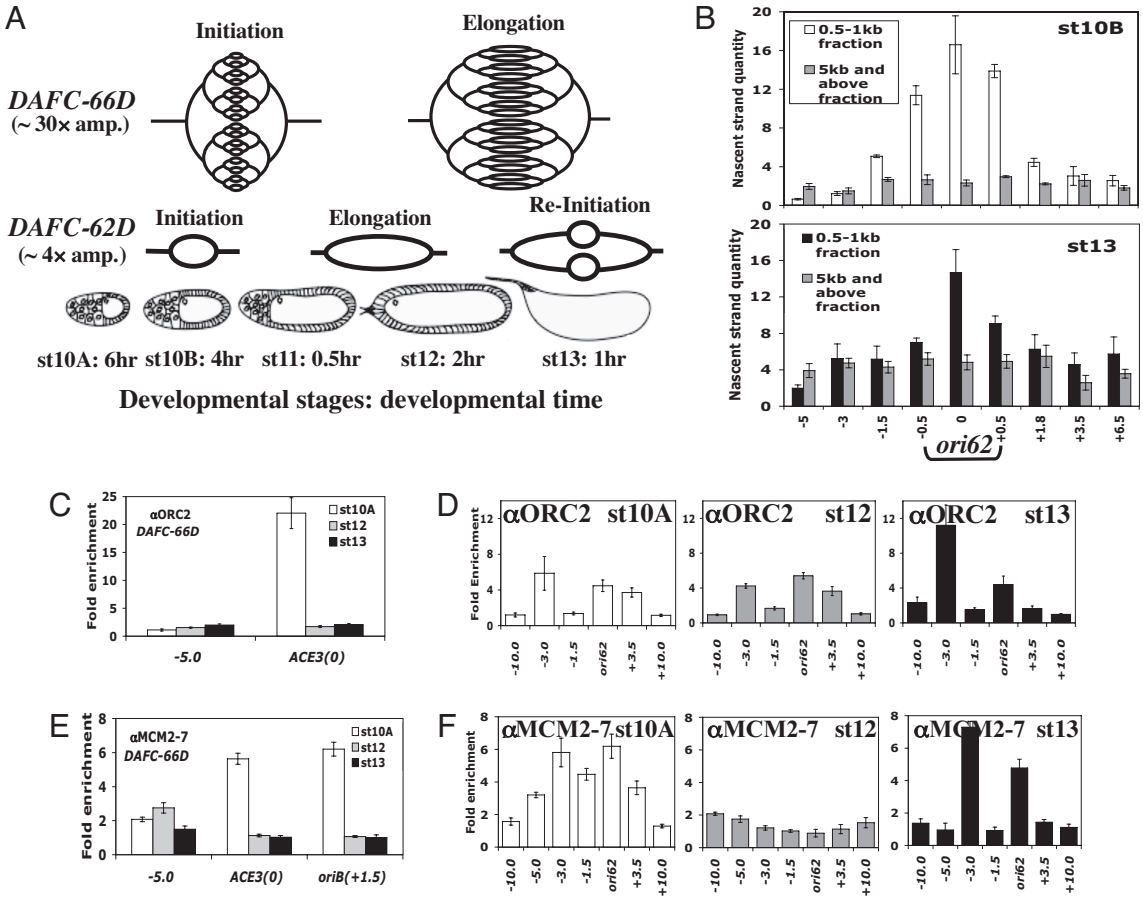

Fig. 1. Mapping the amplification origin and zones of differential association of pre-RC within *DAFC-62D*. (*A*) Timing of egg chamber development and *DAFC* amplification. *DAFC-66D* undergoes five rounds of initiation to reach ~30-fold amplification in stages 10–11, followed by elongation of replication forks in stages 12–13. In *DAFC-62D*, there are two separate rounds of initiation, one in stage 10B, the other stage 13. (*B*) Nascent strand analysis across *DAFC-62D*. Size-fractionated nascent DNA collected from stage 10B or 13 egg chambers was quantified over known serial standards by using real-time PCR. Abundance of nascent DNA (*y* axis, normalized to arbitrary standards) in the 0.5–1 kb and 5 kb above fraction (control) is shown. Numbers on the *x* axis are relative distance away from the central region in kilobases. The 1 kb fragment that confers origin activity is named *ori62*. (*C*) Real-time PCR analysis of ChIP showing enrichment level (± SD) of ORC2 at *ACE3* and a locus 5 kb away over a control locus at *62C5* (15). *ACE3* is specifically pulled down from stage 10A follicular DNA but not later stages. (*D*) Quantitative (real-time) PCR analysis of anti-ORC2 ChIP (± SD) across *DAFC-62D*. The ORC2 association pattern differentially changes from stage 10A, stage 12 to stage 13 of follicle cell development. Numbers on the *x* axis are relative distance away from the center of *ori62* (in kb). Differential MCM ChIP results (± SD) in stages 10A, 12, and 13 across *DAFC-66D* (*E*) and *DAFC-62D* (*F*). Orientation is indicated by + and −. Error bars are standard deviations (SD) of triplicate PCRs.

chamber DNA showed localization of ORC approximately 3 kb away (–3.0) from *ori62* (Fig. 1*D*). ORC also localized 3.5 kb away on the opposite side of *ori62* (+3.5), but only in stage 10A (Fig. 1*D*). Therefore, ORC differentially localized to three zones at *DAFC-62D*, remaining associated with two of them (*ori62* and –3.0) from stage 10A on (Fig. 2*A*).

We also observed by ChIP that the MCM complex was broadly localized around *ori62* in stage 10A (Fig. 1*F*), reflecting its dual role in replication initiation and elongation. In stage 12, MCM2–7 disassociated from the origin (Fig. 1*F*), although ORC remained bound (Fig. 1*D*). Strikingly, the MCM complex was reloaded to *ori62* and −3.0 in stage 13 (Fig. 1*F*). In contrast, at *DAFC-66D*, MCM2–7 associated with *ACE3* and *oriβ* in stage 10A but not afterward (Fig. 1*E*), paralleling the binding pattern of ORC (Fig. 1*C*). This result suggested that at *DAFC-62D* there was developmentally regulated pre-RC binding that used different *cis*-acting elements to direct origin firing in different stages [Fig. 2*A* and supporting information (SI) Fig. S1]. The differential control of pre-RC binding that we observed may be due to specification of *cis* elements and/or *trans* factors such as transcription proteins that could affect ORC binding (10, 13).

ORC-Binding Sequences Are Required for Amplification. We used P-element mediated transformation to test the function of the *cis* elements that associated with the pre-RC *in vivo*, exploiting the Suppressor of Hairy-wing binding sites (SHWBS) insulator to protect the transposon from inhibitory position effects (9) (Fig. 2*B*). We first tested *ori62* alone, but found that in two of two transformation lines, the transposons did not amplify (Fig. 2*D*), indicating the requirement for additional sequences such as enhancer-like *ACE3* elements.

The amplification properties of a 10 kb fragment spanning the maximally amplified region of *DAFC-62D* were tested in P-element transformation lines by FISH/BrdU double labeling and real-time PCR quantification (Fig. 2 *B–D*). In three of three transformation lines tested, the 10 kb fragment amplified at the same levels and developmental times as the endogenous amplicon.

We tested whether the ORC binding zones were required for amplification and found that multiple elements were essential. When either *ori62* (origin) or –3.0 (control element) was deleted from the 10 kb transposon, the remaining sequences did not support detectable amplification, as demonstrated by real-time

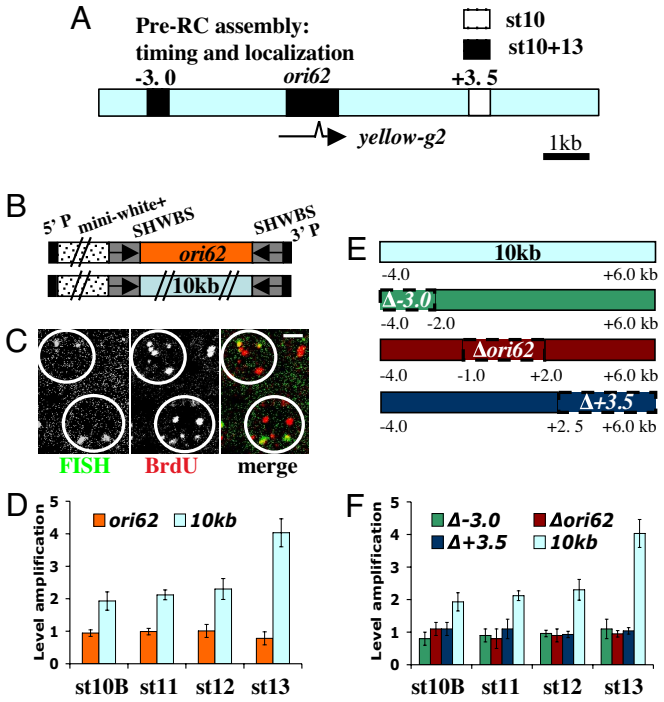

Fig. 2. Genetic analysis of *cis* control elements for *DAFC-62D* amplification. (*A*) Diagram of the 10 kb central amplified fragment in *DAFC-62D* showing the three stage-specific pre-RC zones of localization: *ori62*, −3.0, and +3.5. (*B*) Structure of the transposon construct within the 5′ and 3′ P element sequences. The *miniwhite* gene and 10 kb are not to scale. (*C*) FISH (green) and BrdU (red) double immunofluorescence of stage 10B follicle cells that were transformed with the 10 kb central amplified *DAFC-62D* fragment. The 10 kb fragment was processed into FISH probes. The two FISH signals correspond to the endogenous amplicon and the heterologous transposon. Follice cell nuclei are circled. Scale bar = 1 μm. (*D*) Amplification levels (± SE) of transposons containing *ori62* or the entire 10 kb fragment. (*E*) Size and range of deletions relative to the 10 kb transposon [5′ P, 3′ P, *SHWBS*, and *miniwhite* not shown]. Numbers beneath constructs indicate relative distance (in kb) to the center of *ori62*. (*F*) Amplification level (± SE) of transposons with –3.0, *ori62*, or +3.5 deleted, as compared to the 10 kb transposon. Error bars are standard errors (SE) of analyses of two or three independent transformation lines.

PCR analyses on two or three independent lines for each transposon (Fig. 2 *E* and *F*). Deletion of the +3.5 element also blocked amplification in all developmental stages (Fig. 2*F*). The requirement of +3.5 for stage 13 amplification was unexpected, because +3.5 was only bound by pre-RC in stage 10 (Fig. 2*A*).

The large control region necessary for *DAFC-62D* amplification contrasts with the two small elements of *DAFC-66D*, *ACE3* and *oriβ*, separated by only 1.5 kb and sufficient for proper regulation of amplification. It is, however, analogous to one class of mammalian origins known as large zones of initiation (20). We propose that stage 10 may be the only time window during which ORC loading is permitted and that synergistic recruitment of ORC to all three regions is a prerequisite for later origin firing. Once such window is missed, ORC loading may no longer be possible, providing an explanation for the absence of stage 13 amplification when the stage 10A-specific control element at +3.5 is deleted. It is also possible that the –3.0, +3.5, and *ori62* elements must all be present to form the proper chromatin configuration for replication initiation.

The Two Rounds of Origin Firing at *DAFC-62D* Are Interspersed by Transcription. *ori62* localizes within the transcription unit of the *yellow-g2* (*yg2*) gene (Fig. 2*A*). We did not detect other transcripts in follicle cells on either strand of the 10-kb central amplified region (data not shown). This origin localization is striking, contrasting with the fact that both *ACE3* and *oriβ* are intergenic and upstream of chorion genes (21–23), and, thus, we determined when the *yg2* gene is transcribed relative to the two rounds of origin firing. Nascent *yg2* transcripts were detected as a specific focus in the nucleus by RNA FISH (24, 25), and observed in a narrow time window of early stage 12 (Fig. S1*A*). Slightly later, cytoplasmic *yg2* message began to accumulate, and nuclear staining became undetectable (data not shown). Thus, *yg2* transcription occurs in stage 12, between the two rounds of amplification origin firing.

α-Amanitin Specifically Inhibits *DAFC-62D* Stage 13 Amplification. To investigate potential functional links between transcription and amplification at *DAFC-62D*, we used α-amanitin, an RNAPII inhibitor (26), to block RNAPII elongation. Dissected ovaries were incubated in α-amanitin and allowed to develop *in vitro* for 5 h, the time window that spans stage 10B through 13 under physiological conditions (Fig. 1*A*) (11). The toxin did not affect the developmental programs in general, because the relative abundance of each developmental stage was not significantly changed, and there was apparent progression in development compared with dissected egg chambers that did not undergo *in vitro* culturing (Fig. S2). Such treatment strongly diminished mRNA signals of the chorion gene *Cp38* detected by *in situ* hybridization experiments (data not shown) and completely eliminated the stage 12 FISH spot of nascent *yg2* transcripts (Fig. 3*F*). It also affected the nuclear distribution of RNAPII (*SI Text* and Fig. S1).

We used real-time PCR to measure quantitatively the effects of α-amanitin and found that the stage 13 round of initiation at *DAFC-62D* was specifically inhibited (Fig. 3*C*), whereas initiation in stage 10B was unchanged (Fig. 3*B*). The effect of blocking transcription elongation was specific for the late firing at *DAFC-62D*. The treatment did not change the cumulative amplification levels of *DAFC-66D* in stage 13 (Fig. 3*A*). Furthermore, origin firing in stage 12 at a newly identified amplicon was not affected by α-amanitin (J. Kim, F. Xie, and T. Orr-Weaver, unpublished results). These results suggested that transcription was required specifically for origin activation in stage 13 at *DAFC-62D*.

We examined the effect of α-amanitin on *DAFC-62D* transposons as a further test of whether the requirement for transcription could be a *cis* effect rather than the need to transcribe a gene whose product is required for initiation. Unexpectedly, we observed that three independent transposon insertions carrying the 10 kb fragment from *DAFC-62D* underwent a normal round of amplification in stage 13 in the presence of the toxin (Fig. 3*D*). This result indicated strongly that the inhibition of amplification at *DAFC-62D* was not due to a general block of all amplification initiation in stage 13 imposed by α-amanitin, but rather revealed a specific role of transcription for replication at the endogenous *DAFC-62D* site.

Because all transposons were buffered from position effects by SHWBS, we investigated whether the presence of insulators made amplification of these transposons independent of transcription and, therefore, resistant to α-amanitin. SHWBS recruits the Su(Hw) (Suppressor of Hairy-wing) (27, 28) and additional proteins to form insulator bodies that are not influenced by either positive or negative position effects (29). The $su(Hw)^v/su(Hw)^f$ allele combination eliminates insulator activity (30) and can reduce the amplification level of transposons buffered by SHWBS, if they are inserted at sites subject to negative position effects (9). Transposons containing the 10 kb *DAFC-62D* fragment were crossed into the $su(Hw)^v/su(Hw)^f$ background, and two independent transformation lines displayed proper transposon amplification as determined by real-time PCR analyses (Fig. 3*E*), most likely because their insertion sites were permissive for amplification. One line failed to amplify

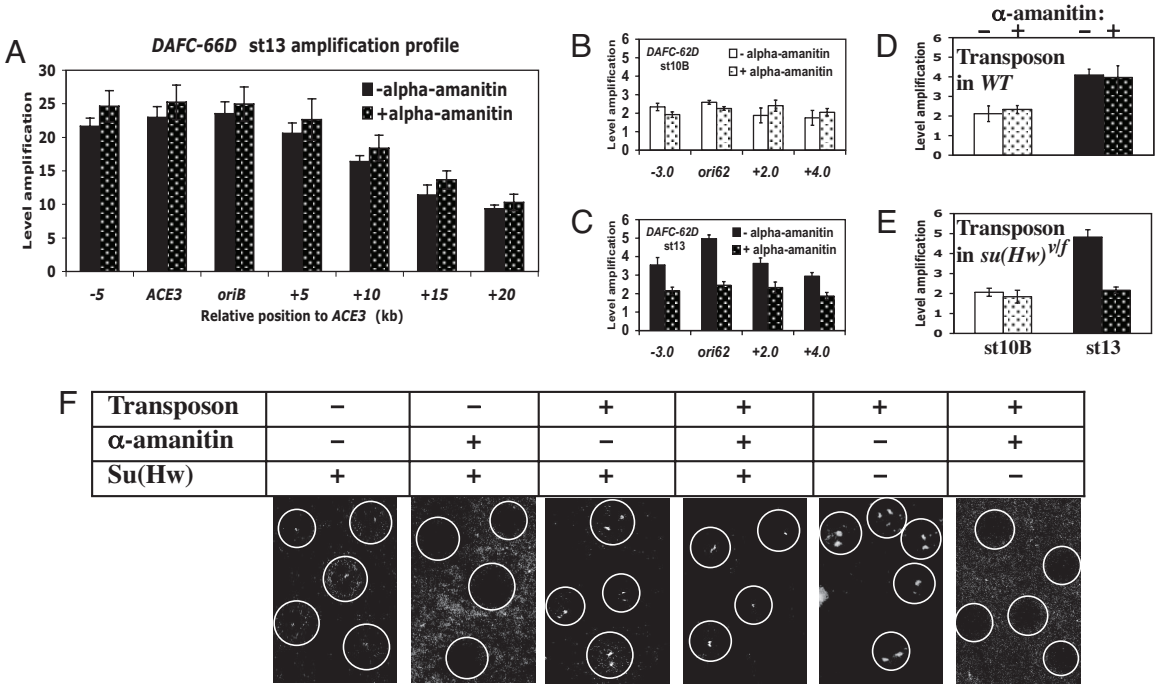

Fig. 3. Effects of α-amanitin on *DAFC-62D* amplification and *yg2* transcription. (*A*) *DAFC-66D* stage 13 amplification level (± SD) with (stippled bars) or without (solid bars) α-amanitin treatment. Comparable profiles suggest no obvious defects in replication, initiation, or elongation, were induced by α-amanitin ($P \geq 0.95$ in Student's T test). Numbers on the *x* axis indicate relative distance to the center of *ACE3* (in kb). (*B*) α-amanitin (stippled bars) did not affect *DAFC-62D* stage 10B (white bars) amplification level (± SD) across the amplicon. Numbers on the *x* axis indicate relative distance to the center of *ori62* (in kb). (*C*) Stage 13 (black bars) amplification of *DAFC-62D* was specifically inhibited by α-amanitin (stippled bars). (*D*) Amplification of the 10 kb transposon was not affected by α-amanitin (stippled bars) in wild-type backgrounds. Three independent transformant lines were analyzed and the amplification levels (± SE) in stages 10B (white bars) and 13 (black bars) at the heterologous loci are shown. (*E*) The 10 kb transposon was sensitive to α-amanitin (stippled bars) in the *su(Hw)* mutant background. Two independent lines from (*D*) were analyzed and amplification level (± SD) for one line is shown. (*F*) Transcription from the endogenous *yg2* locus but not the buffered transposon was inhibited by α-amanitin. Panels show from left to right, respectively, number of RNA FISH signals against *yg2* in stage 12 follicular nuclei: One (no transposon, no α-amanitin), none (no transposon, α-amanitin treated); two (buffered transposon, no α-amanitin), one (buffered transposon, α-amanitin treated); two [$su(Hw)^{-/-}$, transposon, no α-amanitin], and none [$su(Hw)^{-/-}$, transposon, α-amanitin treated]. Images without significant nuclear staining (second and sixth) were overexposed. Nuclei are circled.

in this background (data not shown). Strikingly, in the absence of Su(Hw) insulator function, both transposons became sensitive to α-amanitin, and the stage 13 round of amplification was specifically inhibited (Fig. 3*E*).

We also analyzed transcription of the *yg2* gene on the transposon by RNA FISH. The ectopic copy of *yg2* carried by the transposon was actively transcribed with proper developmental timing, as shown by the appearance of an additional locus of *yg2* nascent transcripts in stage 12 (Fig. 3*F*). After α-amanitin treatment, only one spot of *yg2* transcripts was detectable, presumably from the transposon, because endogenous transcription of *yg2* was completely abolished by α-amanitin in nontransformants (Fig. 3*F*). When the Su(Hw) protein was mutated, transcription in the transposon was blocked by α-amanitin (Fig. 3*F*). These experiments show that neither transcription nor amplification of transposons was inhibited by α-amanitin when buffered by insulators.

The strict correlation between transcription elongation through *yg2* and origin firing in stage 13 raises the possibility that RNAPII elongation is required in *cis* for replication initiation. The alternative is that α-amanitin blocks the transcription of a gene with a product that is essential for stage 13 origin firing at *DAFC-62D*, but not other amplicons. In addition, such a factor would have to be dispensable for activation of *ori-62D* when present on an insulated transposon.

It remains to be determined how RNAPII elongation within an insulated domain occurs even in the presence of α-amanitin. Because functional Su(Hw) protein is required for resistance to α-amanitin, it is likely a consequence of a unique chromatin structure within the "insulator bodies" (29). The inhibition or slowing down of RNAPII by α-amanitin (31) may be minimized by the chromatin environment to allow transcription of *yg2* and the following round of amplification in the presence of the toxin.

Inhibition of Transcription Affects MCM2–7 Localization. ChIP analysis of RNAPII confirmed that α-amanitin treatment affected its distribution across *DAFC-62D*. In untreated follicle cells, RNAPII localized upstream of *yg2*, and after stage 10, also appeared at *ori62* within the coding region of *yg2* (Fig. 4*A* and Fig. S4*A*). The toxin prevented this redistribution into *ori62* from stage 10 to 13, consistent with the finding that it blocks translocation/elongation of RNAPII across *yg2* (Fig. 4*A* and Fig. S4*A*). To investigate the mechanisms by which RNAPII transcription could affect replication, we also analyzed the association of pre-RC components with *DAFC-62D* in the presence of α-amanitin. The binding of ORC2 in stage 10A through 13 was unchanged by the treatment (Fig. S3). The loading of MCM2–7 in stage 13, however, was completely abrogated by α-amanitin, whereas it was unaffected in stage 10 (Fig. 4*B* and Fig. S4*A*).

We next performed sequential ChIP against MCM2–7 and RNAPII to examine whether they co-occupy the same sheared DNA fragments. In stage 13, αMCM2–7 immunocomplexes containing MCM-binding DNA were specifically pulled down by αRNAPII antibody, because in the final ChIP products, there was enrichment of *ori62* and +3.5 (Fig. 4*C* and Fig. S4*B*). The αMCM2–7 supernatant did not contain any RNAPII-bound

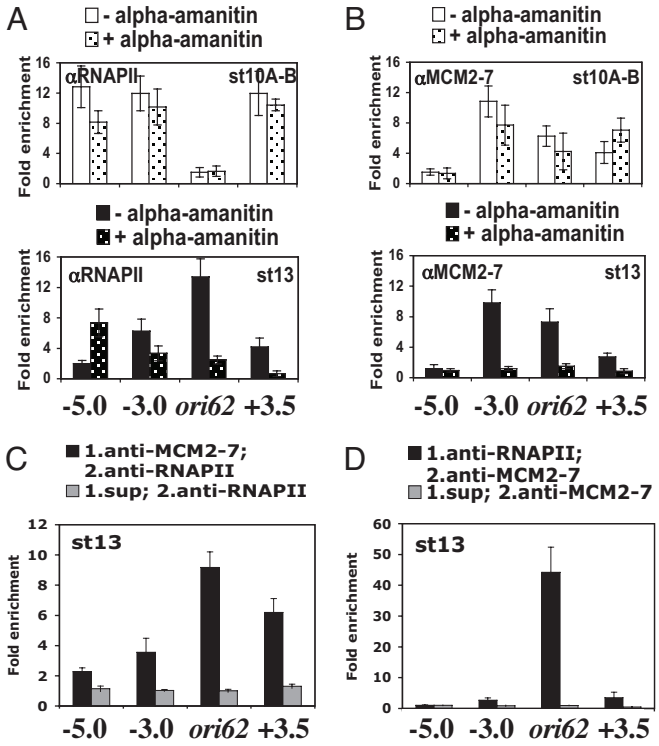

Fig. 4. Association of RNAPII and MCM2–7 with *DAFC-62D* is affected by α-amanitin. (*A*) The effect of α-amanitin on stage 10A-B (approximately half 10A and half 10B combined; *Upper*) and stage 13 (*Lower*) RNAPII binding (± SD) pattern by ChIP. α-amanitin (stippled bars) inhibited the elongation of RNAPII into the *yg2* transcription unit (*ori62*) in stage 13. (*B*) MCM2–7 loading (± SD) in stage 13 (*Lower*) was specifically inhibited by α-amanitin (stippled bars). Stage 10 MCM2-7 localization (*Upper*) was not affected by α-amanitin. (*C*) Sequential ChIP against MCM2–7 followed by RNAPII antibodies suggests that in stage 13 they co-occupy *ori62* and +3.5 specifically. αMCM2–7 supernatant does not contain any RNAPII-bound sequences. (*D*) RNAPII followed by MCM2–7 sequential ChIP strongly suggests their co-localization at *ori62* in stage 13. The –5.0 locus in *DAFC-62D* was used as the denominator when calculating fold enrichment, because the *62C5* control sequence was not detectable in these experiments.

DNA, consistent with MCM2–7 and RNAPII co-occupying the same chromatin. The reciprocal experiment also demonstrated that these proteins associated with the same small pieces of DNA molecules containing *ori62* (Fig. 4*D* and Fig. S4*B*). The sonication protocol resulted in chromatin sizes of 100–500 bp (Fig. S4*C*). These results together strongly indicate that MCM2–7 and RNAPII are in close proximity in *DAFC-62D* in stage 13.

If transcription is needed in *cis* for MCM loading, we envision two candidate molecular mechanisms. Because in stage 13 at *DAFC-62D*, α-amanitin interrupts MCM2–7 loading without affecting the binding of ORC, a special mechanism that involves active transcription via RNAPII may be required to reload MCM2–7 and reactivate *ori62* (Fig. S5). A direct physical interaction has been reported between RNAPII and MCM2–7 in yeast (32, 33), raising the possibility that a RNAPII–MCM2–7 complex serves to load the MCM complex to origins in some developmental contexts. This hypothesis is supported by sequential ChIP results, because RNAPII and MCM2–7 specifically co-occupied the same small pieces of sheared chromatin. An alternative mechanism is that elongation of RNAPII transcription affects chromatin structure and thus MCM loading. RNAPII has been shown to be required for histone displacement ahead of the position of RNAPII within the transcriptionally activated gene's coding region in both yeast and mammalian systems (34–37). A role of RNAPII in displacing proximal histones may play into the successful recruitment of MCM2–7 at the amplification origin (within the *yg2* gene coding region) in *DAFC-62D*.

Conclusions

DAFC-62D differs from other *DAFC*s by undergoing a round of amplification late in follicle cell differentiation, and this difference involves developmental control of ORC and MCM binding (Fig. S5). The late round of origin activation at *DAFC-62D* in stage 13 follicle cells contrasts with the other initiation events in stage 10B in that it takes place at least four hours after the cessation of previous genomic replication. This developmental delay may have created a quiescent (or even inhibitory) state of replication activation in stages 11 and 12 that has to be overcome by unique mechanisms. The analyses of *DAFC-62D* and *−66D* demonstrate that there are distinct mechanisms that differentially regulate amplification origins during *Drosophila* follicle cell development. Our findings reveal pathways to control localization of replication factors, license origins, and activate DNA replication, which provide a conceptual framework for defining how origin selection and activation are regulated by transcription in metazoan development.

Materials and Methods

Plasmid and Transformation Line Construction. All transposon constructs were individually injected into *yw* embryos to establish at least three independent homozygous transformation lines per each construct. At least two lines per each construct were analyzed for amplification level by real-time PCR (see below). Primers targeted transposon-specific sequences to distinguish between the endogenous *DAFC-62D* and the heterologous transposons. Primer sequences are available upon request. To examine the effects of Su(Hw), transposons on either the *X* or *2nd* chromosome were crossed into $y^2\ sc^1\ w^{67}\ ct^6\ f^1$; $bx^{34e}\ su(Hw)^v/TM6$, $su(Hw)^f$, *Ubx* (30).

Chromatin Immunoprecipitation. ChIP was performed on 300 staged egg chambers per experiment as described (18). To immunoprecipitate protein-bound chromatin, 1:250 diluted anti-ORC2 (Steve Bell, MIT), 1:250 anti-RNAPII, or 1:100 diluted anti-MCM2–7 (Steve Bell, MIT) was incubated with chromatin at 4°C overnight. The only RNAPII antibody that worked for ChIP was clone CTD4H8 which recognizes both the phospho and nonphospho carboxyl-terminal domain of RNAPII; other antibodies (H14, 8WG16, and H5) that recognized either form did not yield positive signals (data not shown).

Quantitative (Real-Time) PCR. Absolute quantitative (real-time) PCR was performed as described (14, 15). Standard curves were constructed from four tenfold serial dilutions of stage 1–8 egg chamber DNA (for amplification level), BACR22J16 DNA (for nascent strand analysis, see below), or input chromatin before immunoprecipitation (for ChIP). The endogenous control was a nonamplified locus at *62C5* (15).

Relative quantitative (real-time) PCR was used to detect the difference between a test sample and a calibrator sample wherever indicated in the text according to manufacturer's recommendations (Applied Biosystems 7300 Fast Real-Time PCR System). The calibrator sample was either stage1–8 egg chamber DNA for amplification profiling, or input chromatin for ChIP assays. The same endogenous control at *62C5* was used (15).

Sequential ChIP. Sequential ChIP was performed as described (38). Comparable amounts of antibodies were used as in single ChIP experiments. Pellets and supernatant from the first IP were both subjected to secondary IP, and resulting DNA samples were analyzed against input chromatin. Enrichment levels were calculated over the common *62C5* control by real-time PCR unless otherwise noted (in Fig. 4*D*).

Nascent Strand Analysis. Staged egg chambers (50–100) were dissected in nonsupplemented Grace's medium (GIBCO-BRL) and immediately frozen in −80°C until accumulatively 1,000 were collected. Stage 13 egg chambers were further manipulated to remove the debris of nurse cells, because these apoptotic cells contain single-stranded DNA and produced high levels of background in previous trials. Nascent DNA isolation and size fractionation were performed as described (39, 40). The only modification was that the gel fractionized DNA was recovered by using the Qiaquick Gel Extraction Kit

(Qiagen) and eluted in 30 μl of TE buffer. Each fraction was individually analyzed for the abundance of specific sequences by absolute quantitative real-time PCR, referenced to serial dilutions of BACR22J16 DNA as standards, with the least concentrated standard sample designated as 1.

α-Amanitin Treatment. Whole ovaries were dissected from female *Oregon R* flies and incubated *in vitro* in 333 μg/ml α-amanitin for 5 h at room temperature as described (11). Dissection in unsupplemented Grace's media is important for successful *in vitro* development of egg chambers. Egg chambers were dissected immediately after incubation and subjected to real-time PCR analysis for amplification level in each stage. For immunofluorescence and ChIP experiments, ovaries were washed and formaldehyde fixed right after α-amanitin treatment.

Transposon Construction. For details of transposon construction see *SI Text*.

ACKNOWLEDGMENTS. We thank David MacAlpine and Stephen Bell for supplying the ORC2 and MCM2–7 antibodies and inspiring discussions, John Tower for providing pCaSpeR-4 constructs, Jacob Mueller for advice on RNA FISH, Bashi Raveendranathan and Anja-Katrin Bielinsky for the nascent strand analysis protocol, Pamela Geyer for *su*(*Hw*) mutant strains, as well as Jianzhu Chen, Troy Littleton, and Julie Claycomb for suggestions. The confocal microscopy was conducted by using the W.M. Keck Foundation Biological Imaging Facility at the Whitehead Institute. Stephen Bell, Peter Reddien, Andreas Hochwagen, Cintia Hongay, Yingdee Unhavaithaya, and Jane Kim provided helpful comments on the manuscript. This work was supported by the National Institutes of Health Grant GM57541 (to T.L.O.-W.).

1. Bell SP (2002) The origin recognition complex: From simple origins to complex functions. *Genes Dev* 16:659–672.
2. Cvetic C, Walter JC (2005) Eukaryotic origins of DNA replication: Could you please be more specific? *Semin Cell Dev Biol* 16:343–353.
3. Jeon Y, *et al.* (2005) Temporal profile of replication of human chromosomes. *Proc Natl Acad Sci USA* 102:6419–6424.
4. Gerbi SA (2005) Mapping origins of DNA replication in eukaryotes. *Methods Mol Biol* 296:167–180.
5. Norio P (2006) DNA replication: The unbearable lightness of origins. *EMBO Rep* 7:779–781.
6. Gilbert DM (2005) Origins go plastic. *Mol Cell* 20:657–658.
7. Claycomb JM, Orr-Weaver TL (2005) Developmental gene amplification: Insights into DNA replication and gene expression. *Trends Genet* 21:149–162.
8. Tower J (2004) Developmental gene amplification and origin regulation. *Annu Rev Genet* 38:273–304.
9. Lu L, Tower J (1997) A transcriptional insulator element, the *su*(*Hw*) binding site, protects a chromosomal DNA replication origin from position effects. *Mol Cell Biol* 17:2202–2206.
10. Royzman I, Austin RJ, Bosco G, Bell SP, Orr-Weaver TL (1999) ORC localization in *Drosophila* follicle cells and the effects of mutations in *dE2F* and *dDP*. *Genes Dev* 13:827–840.
11. Bosco G, Du W, Orr-Weaver TL (2001) DNA replication control through interaction of E2F-RB and the origin recognition complex. *Nat Cell Biol* 3:289–295.
12. Beall EL, Bell M, Georlette D, Botchan MR (2004) Dm-myb mutant lethality in *Drosophila* is dependent upon *mip130*: Positive and negative regulation of DNA replication. *Genes Dev* 18:1667–1680.
13. Beall EL, Manak JR, Zhou S, Bell M, Lipsick JS, Botchan MR (2002) Role for a *Drosophila* Myb-containing protein complex in site-specific DNA replication. *Nature* 420:833–837.
14. Claycomb JM, Benasutti M, Bosco G, Fenger DD, Orr-Weaver TL (2004) Gene amplification as a developmental strategy: Isolation of two developmental amplicons in *Drosophila*. *Dev Cell* 6:145–155.
15. Claycomb JM, MacAlpine DM, Evans JG, Bell SP, Orr-Weaver TL (2002) Visualization of replication initiation and elongation in *Drosophila*. *J Cell Biol* 159:225–236.
16. Giacca M, *et al.* (1994) Fine mapping of a replication origin of human DNA. *Proc Natl Acad Sci USA* 91:7119–7123.
17. Kobayashi T, Rein T, DePamphilis ML (1998) Identification of primary initiation sites for DNA replication in the hamster dihydrofolate reductase gene initiation zone. *Mol Cell Biol* 18:3266–3277.
18. Austin RJ, Orr-Weaver TL, Bell SP (1999) *Drosophila* ORC specifically binds to *ACE3*, an origin of DNA replication control element. *Genes Dev* 13:2639–2649.
19. Landis G, Kelley R, Spradling AC, Tower J (1997) The *k43* gene, required for chorion gene amplification and diploid cell chromosome replication, encodes the *Drosophila* homolog of yeast origin recognition complex subunit 2. *Proc Natl Acad Sci USA* 94:3888–3892.
20. Gilbert DM (2004) In search of the holy replicator. *Nat Rev Mol Cell Biol* 5:848–855.
21. Delidakis C, Kafatos FC (1989) Amplification enhancers and replication origins in the autosomal chorion gene cluster of *Drosophila*. *EMBO J* 8:891–901.
22. Orr-Weaver TL, Spradling AC (1986) *Drosophila* chorion gene amplification requires an upstream region regulating *s18* transcription. *Mol Cell Biol* 6:4624–4633.
23. Heck MM, Spradling AC (1990) Multiple replication origins are used during *Drosophila* chorion gene amplification. *J Cell Biol* 110:903–914.
24. Jolly C, Mongelard F, Robert-Nicoud M, Vourc'h C (1997) Optimization of nuclear transcript detection by FISH and combination with fluorescence immunocytochemical detection of transcription factors. *J Histochem Cytochem* 45:1585–1592.
25. Jolly C, Robert-Nicoud M, Vourc'h C (1998) Contribution of growing RNA molecules to the nuclear transcripts foci observed by FISH. *Exp Cell Res* 238:299–304.
26. Lindell TJ, Weinberg F, Morris PW, Roeder RG, Rutter WJ (1970) Specific inhibition of nuclear RNA polymerase II by alpha-amanitin. *Science* 170:447–449.
27. Spana C, Corces VG (1990) DNA bending is a determinant of binding specificity for a *Drosophila* zinc finger protein. *Genes Dev* 4:1505–1515.
28. Spana C, Harrison DA, Corces VG (1988) The *Drosophila melanogaster* suppressor of Hairy-wing protein binds to specific sequences of the *gypsy* retrotransposon. *Genes Dev* 2:1414–1423.
29. Gerasimova TI, Corces VG (2001) Chromatin insulators and boundaries: Effects on transcription and nuclear organization. *Annu Rev Genet* 35:193–208.
30. Harrison DA, Gdula DA, Coyne RS, Corces VG (1993) A leucine zipper domain of the suppressor of Hairy-wing protein mediates its repressive effect on enhancer function. *Genes Dev* 7:1966–1978.
31. Rudd MD, Luse DS (1996) Amanitin greatly reduces the rate of transcription by RNA polymerase II ternary complexes but fails to inhibit some transcript cleavage modes. *J Biol Chem* 271:21549–21558.
32. Holland L, Gauthier L, Bell-Rogers P, Yankulov K (2002) Distinct parts of minichromosome maintenance protein 2 associate with histone H3/H4 and RNA polymerase II holoenzyme. *Eur J Biochem* 269:5192–5202.
33. Gauthier L, *et al.* (2002) The role of the carboxyterminal domain of RNA polymerase II in regulating origins of DNA replication in *Saccharomyces cerevisiae*. *Genetics* 162:1117–1129.
34. Brown SA, Kingston RE (1997) Disruption of downstream chromatin directed by a transcriptional activator. *Genes Dev* 11:3116–3121.
35. Zhao J, Herrera-Diaz J, Gross DS (2005) Domain-wide displacement of histones by activated heat shock factor occurs independently of Swi/Snf and is not correlated with RNA polymerase II density. *Mol Cell Biol* 25:8985–8999.
36. Lee CK, Shibata Y, Rao B, Strahl BD, Lieb JD (2004) Evidence for nucleosome depletion at active regulatory regions genome-wide. *Nat Genet* 36:900–905.
37. Schwabish MA, Struhl K (2004) Evidence for eviction and rapid deposition of histones upon transcriptional elongation by RNA polymerase II. *Mol Cell Biol* 24:10111–10117.
38. Shang Y, Hu X, DiRenzo J, Lazar MA, Brown M (2000) Cofactor dynamics and sufficiency in estrogen receptor-regulated transcription. *Cell* 103:843–852.
39. Cotterill S (1999) *Eukaryotic DNA replication* : *A practical approach* (Oxford Univ Press, Oxford; New York).
40. Lunyak VV, Ezrokhi M, Smith HS, Gerbi SA (2002) Developmental changes in the Sciara II/9A initiation zone for DNA replication. *Mol Cell Biol* 22:8426–8437.